First-principles study of the (001) surface of cubic $CaTiO_3$

Yuan Xu Wang,[1,2] Masao Arai,[1] Taizo Sasaki,[1] and Chun Lei Wang[2]
[1]*Computational Materials Science Center, National Institute for Materials Science, Tsukuba 305-0044, Japan*
[2]*School of Physics and Microelectronics, Shandong University, Jinan 250100, People's Republic of China*
(Received 20 February 2005; revised manuscript received 11 November 2005; published 6 January 2006)

We present first-principles calculations on the (001) surfaces of cubic $CaTiO_3$ with CaO and TiO_2 terminations. For the TiO_2-terminated surface, the largest relaxation is on the second layer atoms, not on the first layer ones. This behavior is different to $SrTiO_3$ and $BaTiO_3$. The large relaxation of the Ca atoms in the second layer deeply affects the band structure of the TiO_2-terminated surface structure. The results of the surface energy calculations show that the (001) surface of $CaTiO_3$ is most easily constructed among these three materials. The analysis of the relaxed structure parameters reveals that the rumpling of the (001) surface for $CaTiO_3$ is the strongest among the three materials.

DOI: 10.1103/PhysRevB.73.035411 PACS number(s): 68.35.Bs, 68.35.Md, 68.47.Gh

I. INTRODUCTION

The ferroelectric ABO_3 perovskites have been investigated extensively by experimental and theoretical researchers because they have many technological applications such as high-capacity memory cells or optical waveguides. In such devices, the perovskites are typically used in the form of thin films. Therefore, it is important to investigate how the physical properties are affected by surfaces. In recent years, first-principles studies on the surface of ferroelectrics have deeply enhanced the understanding of surface effects on their ferroelectricities and other properties.[1–10]

Among ABO_3 perovskites, surfaces of $SrTiO_3$ and $BaTiO_3$ have been most extensively studied theoretically. The surface relaxations of ideal (001) surfaces have been determined from first-principles calculations with fairly good agreement with experimental observations.[1,2,4–6,8–10] It is found that the most significant relaxation is a rumpling of the topmost surface atoms. The surface relaxation affects the electronic structures, resulting in the appearance of surface states on the TiO_2-terminated surface. The relative stability of different surfaces has been also discussed in the context of thermodynamic equilibrium. Other types of surface such as (110) and (111) have been also studied theoretically.[2,3,7,11]

In the present paper, we only focus on cubic $CaTiO_3$. It has been widely used as an electronic ceramic. It is also a key component of Synroc, a synthetic rock form used to immobilize nuclear waste.[12] Although $ATiO_3$ (A = Sr, Ba, Ca) compounds belong to the same II-IV type perovskite and have a common cubic structure at high temperatures, they show different dielectricity and phase transition behavior. $CaTiO_3$ (Ref. 13) and $SrTiO_3$ are incipient ferroelectrics, while $BaTiO_3$ is a typical ferroelectric. Moreover, the critical temperature of transition from the cubic to low-temperature phase for $CaTiO_3$, 1580 K, is extremely high in comparison with those for $SrTiO_3$ and $BaTiO_3$, 105 K and 393 K, respectively. The high critical temperature for $CaTiO_3$ indicates a remarkable difference in the stability of the cubic phase to $SrTiO_3$ and $BaTiO_3$, and thus it is expected that this difference affects its surface properties. However, in contrast to $SrTiO_3$ and $BaTiO_3$, there is no theoretical study of the surface structure of cubic $CaTiO_3$ by first-principles calculations to our knowledge. Only the semiempirical shell model has been applied to the surface of $CaTiO_3$ by Chen[14] as well as that of $SrTiO_3$ and $BaTiO_3$. Thus, it would be of fundamental importance to study the surface of $CaTiO_3$ theoretically. We chose the (001) surface as a typical nonpolar surface because most previous works on the surface of $SrTiO_3$ and $BaTiO_3$ are of the (001).

We studied the (001) surface of cubic $CaTiO_3$ from first-principles calculations. From these calculations and a comparison with other results for $BaTiO_3$ and $SrTiO_3$, we try to find some rules of surface properties with different A-site atoms in $ATiO_3$ perovskites. By calculating the surface structures of cubic $CaTiO_3$, we show that the surface properties of cubic $CaTiO_3$ are different to those of $SrTiO_3$ and $BaTiO_3$. For the TiO_2-terminated surface of cubic $CaTiO_3$, the largest relaxations occur on the second layer atoms. Moreover, the CaO- and TiO_2-terminated surfaces can equally exist in the (001) surface of cubic $CaTiO_3$, which is different from that of $SrTiO_3$. Regarding the method used in our calculations, details are described in Sec. II. The structure, the density of states (DOS), and the band structure are analyzed in Sec. III. The conclusion is given in the last section.

II. METHOD

The calculations presented in this study were performed within the density functional theory, using the plane-wave pseudopotential method. We used the CASTEP computer code,[15] which implements the method. The generalized gradient approximation[16] (GGA) was used with the ultrasoft pseudopotential.[17] The structure was optimized with the Broyden-Fletcher-Goldfarb-Shanno (BFGS) method,[18] and the forces on each ion were converged to less than 0.03 eV/Å. The pseudopotentials used for bulk and surface slab were constructed by the electron configurations as Ca $3s^2\ 3p^6\ 4s^2$ states, Ti $3s^2\ 3p^6\ 3d^2\ 4s^2$ states, and O $2s^2\ 2p^4$ states. A plane-wave cutoff energy of 340 eV was employed throughout. The calculations were done using a (6,6,1) Monkhorst-Pack mesh which corresponds to six **k** points in the irreducible Brillouin zone. To test the convergence with

respect to the cutoff energy and the **k**-point mesh, we repeated the calculations for a (12,12,1) mesh with cutoff energy of 400 eV. The surface energies differ by less than 2 meV/a_0^2 (where a_0 is our theoretical lattice constant of bulk $CaTiO_3$). The result shows that these cutoff energies and **k** points are enough for this system.

Before starting the surface calculations, we optimized the bulk structure of the cubic phase by the same method and the same computational conditions [the **k**-point mesh was (6,6,6)]. Our theoretical lattice constant a_0 is 3.88 Å, which is only 0.3% smaller than experimental one, 3.8950 Å.[19] We used the theoretical lattice constant in all calculations.

In our calculations, two types of termination were considered: type-I (CaO termination) and type-II (TiO_2 termination) surfaces. The periodic boundary condition was used in calculations with the repeated slab model. For the type-I surface, the slab consists of five CaO and four TiO_2 layers and, for the type-II, five TiO_2 and four CaO layers. For both cases, the slabs with four lattice constants thickness are separated by a 12 Å vacuum region and are tetragonal with space group *P*4*mmm*. During the surface structure optimization, all atoms were fully relaxed. Increasing the number of layers to 11 only make a difference in the value of *s* (defined below) 2.7% for the CaO-terminated surface of $CaTiO_3$.

III. RESULTS AND DISCUSSIONS

A. Surface energies

As long as the surface is in equilibrium with its surroundings (TiO_2 and CaO), the surface stability can be determined from the grand thermodynamic potential F as a function of the chemical potentials of TiO_2 and CaO, μ_{TiO_2} and μ_{CaO}, respectively.[5,20] In principle, F should be a function of the chemical potentials for Ca, Ti, and O_2, respectively. Since Ca and Ti are easily oxidizable, we just define F as a function of the chemical potentials of their oxides for each type as

$$F(\text{I or II}) = \frac{1}{2}[E_{\text{slab}}(\text{I or II}) - N_{TiO_2}(\mu_{TiO_2} + E_{TiO_2}) - N_{CaO}(\mu_{CaO} + E_{CaO})], \quad (1)$$

where E_{slab}, E_{TiO_2}, and E_{CaO} are the total energies of the relaxed surface structure, TiO_2 in the rutile structure, and CaO in the rocksalt structure, respectively. N_{TiO_2} and N_{CaO} are the number of TiO_2 and CaO layers in surfaces structures. For the type-I surface, N_{TiO_2} and N_{CaO} are 4 and 5, respectively. N_{TiO_2} and N_{CaO} are 5 and 4 for the type-II one. The surface of $CaTiO_3$ can be stable, whichever the surface type is, under the conditions of

$$-E_f = \mu_{TiO_2} + \mu_{CaO} \quad (2)$$

and

$$-E_f \leqslant \mu_{TiO_2}, \mu_{CaO} \leqslant 0, \quad (3)$$

where E_f is the formation energy (per formula unit) of cubic bulk $CaTiO_3$ from rocksalt CaO and rutile TiO_2:

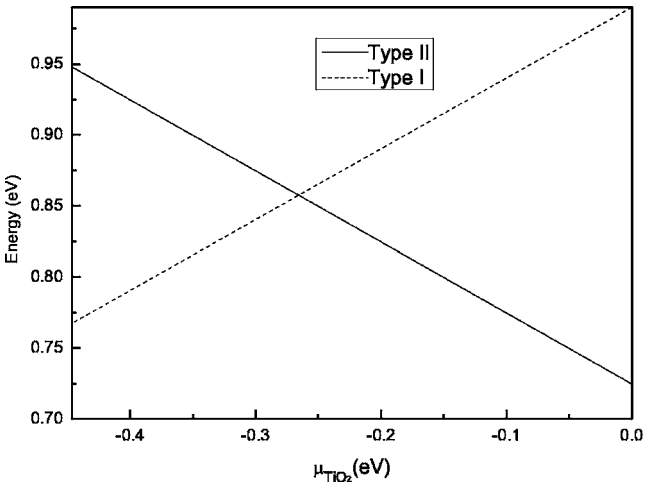

FIG. 1. Grand thermodynamic potential F as a function of the chemical potential of TiO_2, μ_{TiO_2}, for the two types of surfaces of $CaTiO_3$.

$$-E_f = E_{CaTiO_3} - E_{CaO} - E_{TiO_2}, \quad (4)$$

where E_{CaTiO_3} is the total energy per formula unit of cubic $CaTiO_3$.

Figure 1 shows our calculated F for the surface structure of $CaTiO_3$. Our calculated formation energy of cubic $CaTiO_3$ is 0.45 eV. This small formation energy comes from the fact that the cubic structure is not the lowest-energy structure for $CaTiO_3$. Indeed, we found that the distorted structure with orthorhombic *Pbnm* (Ref. 19) has lower energy (about 1.5 eV from our calculation). From Fig. 1, we can see that the two types of surface termination have a comparable range of thermodynamic stability which means that either a type-I or type-II surface could be formed depending on whether growth occurs in Ca-rich or Ti-rich conditions.

We also performed the same calculations for $SrTiO_3$ for comparison, and the result is shown in Fig. 2. In our calculations for $SrTiO_3$, a similar structure model was used: The

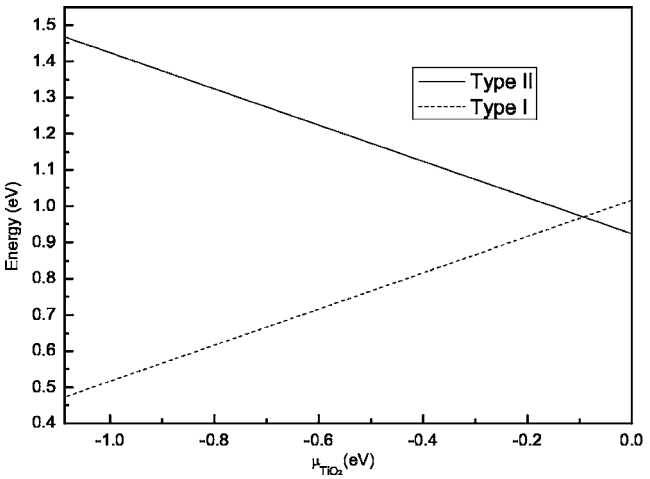

FIG. 2. Grand thermodynamic potential F as a function of the chemical potential of TiO_2, μ_{TiO_2}, for the two types of surfaces of $SrTiO_3$.

TABLE I. Theoretical average surface energies for $CaTiO_3$, $SrTiO_3$, and cubic $BaTiO_3$ (in eV/a_0^2). The E_{cle} means the cleavage energy and the E_{rel} is the relaxation energy.

	E_{cle}	E_{rel}(I)	E_{rel}(II)	E_s
$CaTiO_3$	1.18	−0.42	−0.23	0.86
$SrTiO_3$	1.16	−0.20	−0.18	0.97
$SrTiO_3$[a]		−0.3	−0.14	1.21
$BaTiO_3$	1.13	−0.08	−0.20	0.99
$BaTiO_3$[b]				1.24

[a]Reference 4.
[b]Reference 5.

slab of type-I surface consists of five SrO and four TiO_2 layers and, for the type-II, five TiO_2 and four SrO layers. Moreover, the total energies were calculated with relaxed cubic $SrTiO_3$, rocksalt SrO, and rutile TiO_2. From Fig. 2, it can be seen that the type-I surface is more stable than the type-II one in a wide range of μ_{TiO_2}. Compared to $CaTiO_3$, this behavior is different.

The surface stability of cubic $SrTiO_3$ has been studied by Padilla and Vanderbilt[21] with a similar approach. They have shown that the two types of surface are comparably stable, which is different from the present result. This difference seems attributed to the calculated formation energies for $SrTiO_3$, which is not shown in their paper but can be estimated as 3.2 eV from the range of chemical potential presented in Fig. 1 of Ref. 21. Our calculated formation energy of $SrTiO_3$ is 1.09 eV which is smaller than their value. In order to know whether the disagreement of calculated formation energies is due to the difference between the GGA and local density approximation (LDA), we also calculated the formation energy for $SrTiO_3$ by the LDA with the same computational conditions. Our calculated formation energy is 1.39 eV. This value is similar to that of the GGA and almost same as that reported by Johnston *et al.*[22] within the LDA.

We define E_s to be the average surface energy of two types of surface termination:

$$E_s = F\frac{1}{4}[E_{slab}(\mathrm{I}) + E_{slab}(\mathrm{II}) - 9E_{bulk}], \tag{5}$$

where E_{slab} (I), E_{slab} (II), and E_{bulk} are the total energies of the relaxed type-I slab, the relaxed type-II slab, and the bulk crystal per unit cell, respectively. Since the average surface energy is independent of μ_{TiO_2}, it is suitable for comparisons. Table I illustrates the average surface energy, the cleavage energy and the relaxation energy of $CaTiO_3$, together with those for $SrTiO_3$ (Ref. 4) and $BaTiO_3$ (Ref. 5). The cleavage energy (E_{cle}) and the relaxation energy (E_{rel}) are defined as

$$E_{cle} = \frac{1}{4}[E_{slab}^{(unrel)}(\mathrm{I}) + E_{slab}^{(unrel)}(\mathrm{II}) - 9E_{bulk}], \tag{6}$$

$$E_{rel}(\mathrm{I}) = \frac{1}{2}[E_{slab} - E_{slab}^{(unrel)}(\mathrm{I})], \tag{7}$$

where $E_{slab}^{(unrel)}$ (I), $E_{slab}^{(unrel)}$ (II), and E_{slab} (I) are the total energies for the unrelaxed type-I slab, the unrelaxed type-II slab, and the relaxed type-I slab, respectively. From Table I, we can see that the cleavage energies of the three materials are similar. The relaxation energies of the type-II surface for the three materials are also similar, while those of the type-I surface are very different. The absolute value of the relaxation energy of $CaTiO_3$ is the largest one among the three materials. Thus, the surface energy of $CaTiO_3$ is smaller than that of $SrTiO_3$ and the surface energy of $BaTiO_3$ is the largest. The smaller surface energy means easier cleavability under the condition that migration of atoms can be neglected. Thus, among these materials, the surface of $CaTiO_3$ is the most easily constructed. Chen[14] calculated the (001) surface of $CaTiO_3$, $SrTiO_3$, and $BaTiO_3$ by the shell model and gave the result of the surface energy for these three materials. Its definition of the surface energy is, however, not known and a comparison with it is difficult. Even by the same shell-model method, the surface energy of $SrTiO_3$ by Chen[14] is different from that of other groups.[23]

Recently, it has been reported that perovskite surfaces exhibit multiple surface reconstruction depending on the experimental conditions such as the chemical potential of oxygen, pressure, and temperature. Such reconstructions are beyond our present study. If they are included in the calculations, they may alter the stability of surfaces. It would be desirable to study the detailed reconstruction in future.

TABLE II. Calculated atomic displacements (relative to ideal position) for the CaO- and TiO_2-terminated surfaces. Units are relative to the theoretical lattice constant (a_0=3.88158 Å).

Layer	CaO terminated	δ_z	TiO_2 terminated	δ_z
1	Ca	−0.088	Ti	−0.029
	O	0.007	O	−0.005
2	Ti	0.027	Ca	0.077
	O	0.012	O	0.008
3	Ca	−0.032	Ti	−0.009
	O	−0.001	O	−0.009
4	Ti	0.004	Ca	0.006
	O	−0.001	O	−0.002

B. Structure relaxation

A good agreement in the surface rumpling parameters of $SrTiO_3$ between the DFT calculations[1,4] and the experimental results[24,25] has shown that density functional theory (DFT) calculations can predict well the surface structure of perovskite materials. Table II illustrates our calculated atomic relaxations for the type-I and type-II surface structures of cubic $CaTiO_3$. It can be seen that, for the type-I surface with CaO termination, the Ca atoms move inward (towards the bulk) and the Ti atoms move outward (towards the vacuum). The largest relaxation is on the first layer atoms, as expected. The structure of the $SrTiO_3$ and $BaTiO_3$ (001) surface with full relaxation has been studied.[1,5] The relaxation behavior for the type-I surface of $CaTiO_3$ is similar to those results except the magnitude of displacement: The Ca atoms in the first layer move inward about 8.8% of the bulk lattice constant a_0,

TABLE III. Surface relaxation parameters (in Å) for $CaTiO_3$, $SrTiO_3$ Ref. 1 and $BaTiO_3$ Ref. 5.

	s	Δd_{12}	Δd_{23}
AO terminated			
$CaTiO_3$	0.37	−0.44	0.22
$SrTiO_3$	0.23	−0.28	0.13
$SrTiO_3$[a]	0.20	−0.26	0.11
$BaTiO_3$	0.1	−0.17	0.08
$BaTiO_3$[b]	0.055	−0.146	0.059
TiO_2 terminated			
$CaTiO_3$	0.13	−0.41	0.33
$SrTiO_3$	0.12	−0.24	0.12
$SrTiO_3$[a]	0.09	−0.26	0.18
$BaTiO_3$	0.11	0.23	0.13
$BaTiO_3$[b]	0.1	−0.234	0.079

[a]Reference1.
[b]Reference5.

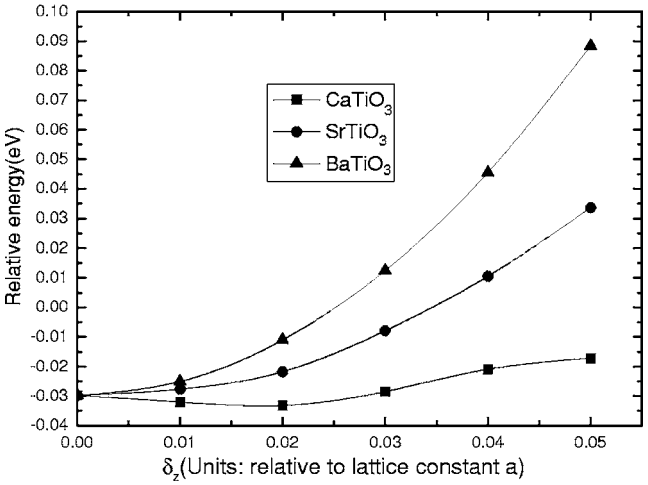

FIG. 3. The total energy as a function of displacement δz of A atoms along the [001] direction for cubic $ATiO_3$ (A=Ca, Sr, and Ba). The lines with solid squares, circles, and triangles represent the results for $CaTiO_3$, $SrTiO_3$, and $BaTiO_3$, respectively.

while the displacement of the Sr and Ba atoms in the first layer are about 5.7% and 2.8%, respectively.

For the type-II surface structure, $CaTiO_3$ has a very different relaxation behavior compared to $SrTiO_3$ and $BaTiO_3$. The largest relaxations can be seen in the second-layer atoms, not in the first-layer atoms. The displacement of the Ca atoms in the second layer is outward about 7.7% and that of the Ti atoms in the first layer is inward about 2.9%. In contrast, for the type-II surface of $BaTiO_3$ and $SrTiO_3$, the largest relaxations are in the first-layer atoms. The displacement of the O atoms is very small in all layers and less than 1%. Moreover, the relaxation direction of the O atoms in the second layer, the outward movement, is opposite to that of $SrTiO_3$ and $BaTiO_3$. Such a different relaxation direction may arise from the large displacement of the Ca atoms in the second layer. The relaxation of the fourth layer for the two types of the surface is less than 0.6%.

In Table III, we present the calculated structural parameters of $CaTiO_3$, $SrTiO_3$, and $BaTiO_3$ and a comparison with those reported previously.[1,5] The quantity s measures the outward displacement of the first-layer oxygen with respect to the first-layer metal atoms, Δd_{12} is the change of the first interlayer spacing, as measured from the surface to the subsurface metal z coordinate, and a similar definition is given to Δd_{23} between the second and third layers. For $SrTiO_3$ and $BaTiO_3$, our results are similar to previous calculated results.[1,5] From Table III, the absolute values of s and Δd for the type-I surface become larger in order of $BaTiO_3$, $SrTiO_3$, and $CaTiO_3$. It means that the rumpling of the type-I surface becomes stronger in this order. For the type-II surface, Δd for these three materials have similar behavior with the type-I surface and the variation of the s value is small. The s value of $SrTiO_3$ is smaller than that of $BaTiO_3$. The s value of $CaTiO_3$ is still the largest one. Since the first layer is TiO_2 for the type-II surface, the s value does not reflect the rumpling of the AO layers. The second layer (AO layer) relaxation behavior shows the rumpling of the AO layers. Thus, we can conclude that the rumpling of the topmost AO layers in the (001) surface structure for $CaTiO_3$ is larger than that in $SrTiO_3$ and $BaTiO_3$ for both types of surface.

In order to understand why the displacement of the Ca atoms is the largest among these three materials during the surface rumpling, we calculated the total energies of the bulk and surface systems of $CaTiO_3$ and $SrTiO_3$ with different A-atom displacements. Figure 3 shows the total energy of cubic $CaTiO_3$, $SrTiO_3$, and $BaTiO_3$ as a function of displacement of the A atoms in the [001] direction, which indicates a distortion from cubic symmetry. From this figure, we can see that the total energy of $CaTiO_3$ decreases for a small displacement of Ca atoms while other compounds exhibit an increase. Thus, for bulk systems the Ca atoms are energetically the easiest to be displaced. This instability of the Ca atoms at the symmetric point is related to the instability of the cubic phase at low temperature.

The total energy changes of the $CaTiO_3$ and $SrTiO_3$ surfaces with the AO termination as a function of the A-atom displacement are given in Fig. 4. From this figure, it can be seen that the total energy of $CaTiO_3$ surface decreases more largely than that of $SrTiO_3$ with the same displacement of A atoms. It means that the Ca atoms can be moved more easily. Thus, the total energy behavior of both bulk and surface structures shows that the Ca atoms have more space for relaxation. The Goldschmidt radii of the Ca, Sr, and Ba atoms in $ATiO_3$ systems are 1.16, 1.37, and 1.52, respectively.[26] They show that the Ca atoms has the largest free space among these three atoms in $ATiO_3$ systems.

Theoretically, the total energy calculations of $CaTiO_3$, $SrTiO_3$, and $BaTiO_3$ for the unrelaxed and relaxed type-II surfaces have shown that the decreasing trend in the electrostatic energy composed of the interaction between nuclei and electron charge of $CaTiO_3$ is larger than those of $SrTiO_3$ and $BaTiO_3$. Thus, the large displacement of Ca atoms in the second layer of type-II surfaces maybe comes from the large decreasing of the electrostatic energy during surface relaxation.

Our calculations show that the Ti, Ca, and O atoms in the ionic states display very different displacements from their

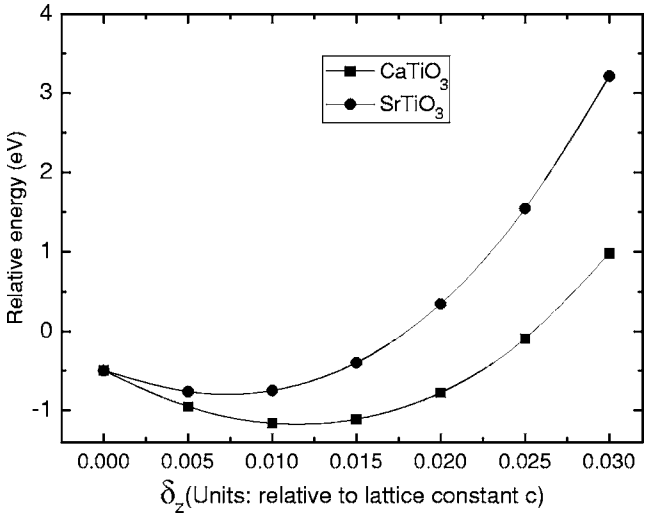

FIG. 4. The total energy as a function of displacement δz of A atoms along the [001] direction for the surface of $CaTiO_3$ and $SrTiO_3$. The lines with solid squares and circles represent the results for $CaTiO_3$ and $SrTiO_3$, respectively.

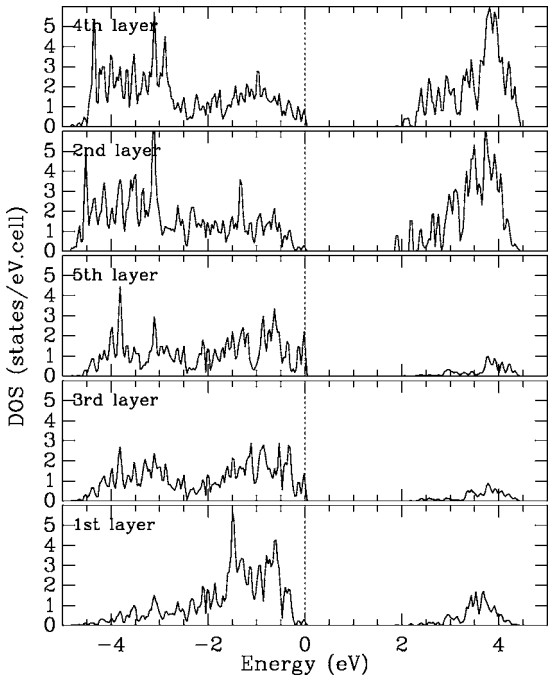

FIG. 6. PDOS decomposed into each layer of the CaO-terminated surface. Individual states are broadened with the width of 0.05 eV.

perfect-crystalline sites. This can lead to the formation of a dipole moment at the surface layers, which are perpendicular to the surface. For the type-I surface, the dipole moment is mainly due to the larger inward displacement of the Ca ions and relative small outward displacement of the O ions. The outward displacement of the Ti ions in the subsurface layer may weakly reduce the large dipole moment formed by the Ca ions displacement. For the type-II surface structure, a dipole moment comes dominantly from the larger outward displacement of the Ca ions and relative small outward displacement of the O ions in the second layer. The inward displacement of the Ti ions in the first layer may partially reduce the dipole moment formed by the Ca-ion displacement. This large surface polarization in $CaTiO_3$ indicates the appearance of a significant electric field near the surface of the cubic crystal and affects the band structure as will be described later.

C. Surface electronic structure

1. Type-I surface

We performed GGA calculations of the electronic structure for bulk and two types of the surface. The bulk band gap was calculated to be 1.95 eV, which is smaller than the experimental value, 3.5 eV. This difference is typical for the GGA calculations. Figure 5 gives the calculated electronic band structures for $CaTiO_3$: (a) surface-projected bulk band structure, (b) the unrelaxed CaO-terminated surface, and (c) the relaxed CaO-terminated surface. It is found that the structure relaxation does not influence the band structure significantly. The calculated band gap for the relaxed CaO-terminated surface is 1.82 eV. Thus, the band gap of the CaO-terminated surface is reduced slightly. The bulk and surface energy bands look similar, and it is difficult to distinguish the surface states. The partial densities of states (PDOS) of different layers for the CaO-terminated surface structure are given in Fig. 6. In this figure, the fifth layer is a central layer and may be regarded as those in the bulk. Comparing with the fifth layer, the amplitude of PDOS from −2 to 0 eV increases in the first layer. The PDOS of the third layer is similar to that of the fifth layer.

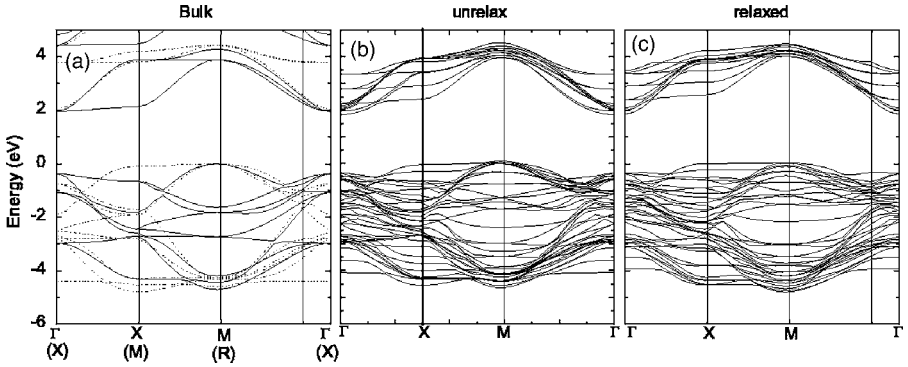

FIG. 5. Calculated electronic band structures for $CaTiO_3$. (a) Projected bulk band structure. The solid and dotted lines represent the band structure on the $\Gamma \rightarrow X \rightarrow M \rightarrow \Gamma$ and $X \rightarrow M \rightarrow R \rightarrow X$ axes, respectively, in the bulk Brillouin zone. (b) The unrelaxed CaO-terminated surface. (c) The relaxed CaO-terminated surface. The top of the occupied states is set to be zero for all cases.

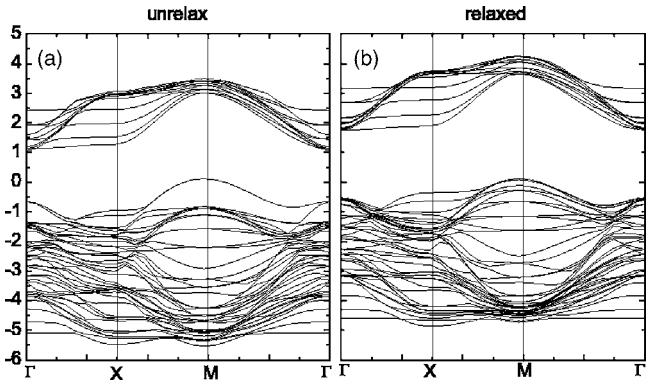

FIG. 7. Calculated electronic band structures for the unrelaxed (a) and the relaxed (b) TiO_2-terminated surface of $CaTiO_3$. The top of the occupied states is set to be zero for both cases.

2. Type-II surface

Figure 7 shows the calculated electronic band structures for the unrelaxed (a) and the relaxed (b) TiO_2-terminated surface of $CaTiO_3$. The PDOS of the relaxed surface is illustrated in Fig. 8. The change in the band structure due to the relaxation is prominent at around the *M* point. The calculated band gap for the relaxed type-II surface is 1.75 eV, which is reduced about 0.2 eV from that of the unrelaxed one. This reduction is smaller than those for $SrTiO_3$ (about 0.7 eV) and $BaTiO_3$ (about 1 eV). In order to know whether the large displacements (compared with Sr and Ba) of the Ca atoms in the second layer affects the band gap of the type-II surface of $CaTiO_3$, we calculated the band structure for a model surface where we moved the Ca atoms in the second layer from the optimized position to 3% of a_0 inward (relative to the unrelaxed position), which is similar to the Sr atoms in the second layer of the type-II surface structure for $SrTiO_3$. The calculated band gap is 0.42 eV. Compared with the gap of the optimized structure, this value is very small. From the above analysis, we can conclude that the large relaxations of the Ca atoms in the second layer affect the O *p* electrons in the first layer and make the band gap of the type-II surface of $CaTiO_3$ large. Compared with $SrTiO_3$ and $BaTiO_3$, such behavior is very different and interesting.

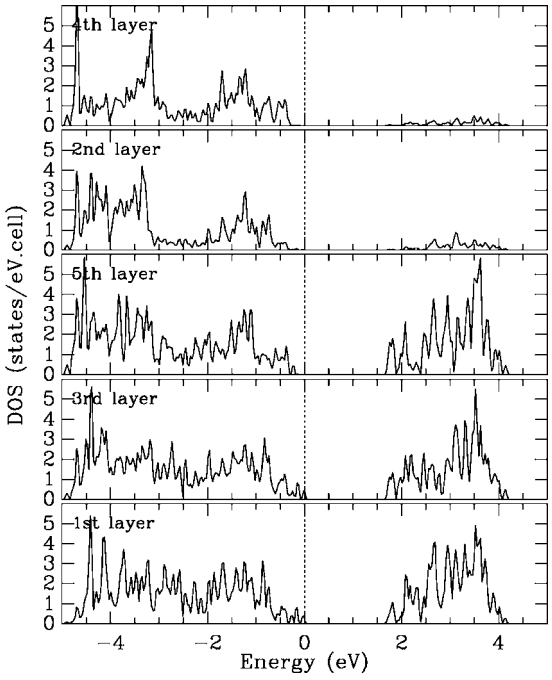

FIG. 8. PDOS decomposed into each layer of the TiO_2-terminated surface $CaTiO_3$, drawn in a manner to Fig. 6.

From Fig. 7(b), it seems that the valence band exhibits an upward shift intruding into the lower part of the band gap, especially at the *M* point. The surface states may be also identified from the PDOS plotted in Fig. 8. In this figure, the fifth layer is a central one and the Ti and O atoms in this layer can be regarded as those in bulk. In fact, the PDOS of the fifth layer has the energy gap similar to that of bulk. The first and third layers show noticeable PDOS up to about 0.2 eV higher in energy. From this comparison, it is considered that surface states appear at the *M* point. The upward shift of the valence band at the TiO_2-terminated surface can be seen in the large enhancement of PDOS of the first and third layers between −1 and 0 eV.

IV. CONCLUSION

The structural and electronic properties of the CaO- and TiO_2-terminated (001) surfaces of cubic $CaTiO_3$ were calculated by the plane-wave pseudopotential method within the GGA. The results were compared to those of $SrTiO_3$ and $BaTiO_3$. We find that, for the TiO_2-terminated surface, the largest relaxation occurs in the second-layer atoms, not in the first-layer ones, which is different from $SrTiO_3$ and $BaTiO_3$. The large displacement of the Ca atoms in the second layer deeply affects the band structure of the TiO_2-terminated surface structure. The calculated surface energies show that the (001) surface of $CaTiO_3$ is most easily created among these three materials. From an analysis of the structure relaxation parameters, we can conclude that the surface rumpling of $CaTiO_3$ is the most significant among these three materials, which is mainly due to its largest decrease in the electrostatic energy during the surface relaxation. The reduction of the electronic band gap for the TiO_2-terminated surface is mainly attributed to the valence-band states of O 2*p* in the first and third layers. The TiO_2-terminated and CaO-terminated surfaces equally exist in the (001) surface.

ACKNOWLEDGMENTS

This work is supported by the National Natural Science Foundation of China under Project No. 10474057.

[1] A. Asthagiri and D. S. Sholl, J. Chem. Phys. **116**, 9914 (2002).
[2] A. Asthagiri and D. S. Sholl, Surf. Sci. **581**, 66 (2005).
[3] A. Asthagiri, C. Niederberger, A. J. Francis, L. M. Porter, P. A. Salvador, and D. S. Sholl, Surf. Sci. **537**, 134 (2003).
[4] C. Cheng, K. Kunc, and M. H. Lee, Phys. Rev. B **62**, 10409 (2000).
[5] J. Padilla and D. Vanderbilt, Phys. Rev. B **56**, 1625 (1997).
[6] V. Ravikumar, D. Wolf, and V. P. Dravid, Phys. Rev. Lett. **74**, 960 (1995).
[7] E. Heifets, W. A. Goddard III, E. A. Kotomin, R. I. Eglitis, and G. Borstel, Phys. Rev. B **69**, 035408 (2004).
[8] R. E. Cohen, J. Phys. Chem. Solids **57**, 1393 (1996).
[9] E. Heifets, S. Dorfman, D. Fuks, and E. Kotomin, Thin Solid Films **296**, 76 (1997).
[10] X. Y. Xue, C. L. Wang, and W. L. Zhong, Surf. Sci. **550**, 73 (2004).
[11] E. Heifets and E. Kotomin, Thin Solid Films **358**, 1 (2000).
[12] A. E. Ringwood, S. E. Kesson, K. D. Reeve, D. M. Levins, and E. J. Ramm, *Radioactive Waste Forms for the Future* (Elsevier, Amsterdam, 1988).
[13] Y. X. Wang, W. L. Zhong, C. L. Wang, and P. L. Zhang, Solid State Commun. **117**, 461 (2001).
[14] S. P. Chen, J. Mater. Res. **13**, 1848 (1998).
[15] M. D. Segall, P. L. D. Lindan, M. J. Probert, C. J. Pickard, P. J. Hasnip, S. J. Clark, and M. C. Payne, J. Phys.: Condens. Matter **14**, 2717 (2002).
[16] J. P. Perdew, K. Burke, and M. Ernzerhof, Phys. Rev. Lett. **77**, 3865 (1996).
[17] D. Vanderbilt, Phys. Rev. B **41**, R7892 (1990).
[18] T. H. Fischer and J. Almlof, J. Phys. Chem. **96**, 9768 (1992).
[19] B. J. Kennedy, C. J. Howard, and B. Chakoumakos, J. Phys.: Condens. Matter **11**, 1479 (1999).
[20] G. X. Qian, R. M. Martin, and D. J. Chadi, Phys. Rev. B **38**, 7649 (1988).
[21] J. Padilla and D. Vanderbilt, Surf. Sci. **418**, 64 (1998).
[22] K. Johnston, M. R. Castell, A. T. Paxton, and M. W. Finnis, Phys. Rev. B **70**, 085415 (2004).
[23] E. Heifets, E. A. Kotomin, and J. Maier, Surf. Sci. **462**, 19 (2000).
[24] N. Bickel, G. Schmidt, K. Heinz, and K. Müller, Phys. Rev. Lett. **62**, 2009 (1989).
[25] N. V. Krainyukova and V. V. Butskii, Surf. Sci. **454**, 628 (2000).
[26] H. D. Megaw, Proc. Phys. Soc. London **58**, 10 (1946).